Since January 2020 Elsevier has created a COVID-19 resource centre with free information in English and Mandarin on the novel coronavirus COVID-19. The COVID-19 resource centre is hosted on Elsevier Connect, the company's public news and information website.

Available online at www.sciencedirect.com
ScienceDirect
Antiviral Research 75 (2007) 179–187
Antiviral Research
www.elsevier.com/locate/antiviral

Plant lectins are potent inhibitors of coronaviruses by interfering with two targets in the viral replication cycle

Els Keyaerts [a], Leen Vijgen [a], Christophe Pannecouque [b], Els Van Damme [c], Willy Peumans [c], Herman Egberink [d], Jan Balzarini [b,*], Marc Van Ranst [a,**]

[a] *Laboratory of Clinical & Epidemiological Virology, Department of Microbiology & Immunology, Rega Institute for Medical Research, University of Leuven, Minderbroedersstraat 10, 3000 Leuven, Belgium*
[b] *Laboratory of Virology and Chemotherapy, Rega Institute for Medical Research, University of Leuven, Belgium*
[c] *Department of Molecular Biotechnology, University of Gent, Belgium*
[d] *Department of Infectious Diseases & Immunology, Veterinary Faculty, Utrecht, The Netherlands*

Received 19 December 2006; accepted 5 March 2007

Abstract

We describe the antiviral activity of plant lectins with specificity for different glycan structures against the severe acute respiratory syndrome coronavirus (SARS-CoV) and the feline infectious peritonitis virus (FIPV) *in vitro*. The SARS-CoV emerged in 2002 as an important cause of severe lower respiratory tract infection in humans, and FIPV infection causes a chronic and often fatal peritonitis in cats. A unique collection of 33 plant lectins with different specificities were evaluated. The plant lectins possessed marked antiviral properties against both coronaviruses with EC_{50} values in the lower microgram/ml range (middle nanomolar range), being non-toxic (CC_{50}) at 50–100 μg/ml. The strongest anti-coronavirus activity was found predominantly among the mannose-binding lectins. In addition, a number of galactose-, *N*-acetylgalactosamine-, glucose-, and *N*-acetylglucosamine-specific plant agglutinines exhibited anti-coronaviral activity. A significant correlation (with an *r*-value of 0.70) between the EC_{50} values of the 10 mannose-specific plant lectins effective against the two coronaviruses was found. In contrast, little correlation was seen between the activity of other types of lectins. Two targets of possible antiviral intervention were identified in the replication cycle of SARS-CoV. The first target is located early in the replication cycle, most probably viral attachment, and the second target is located at the end of the infectious virus cycle.

Keywords: Coronavirus; Plant lectins; Antiviral; SARS-CoV; Mannose

1. Introduction

The identification of a novel coronavirus as the causative agent of the severe acute respiratory syndrome (SARS) has led to a renewed interest in coronaviruses (Rota et al., 2003). Coronaviruses are large, enveloped single-stranded positive sense RNA viruses with a genome of approximately 30 kb in length, the largest found in any of the RNA viruses. Coronaviruses are classified into three groups based on genetic and serological relationships (Gonzalez et al., 2003). The feline infectious peritonitis virus (FIPV) belongs to group 1 and the SARS-CoV is not assigned to any of these groups but is most closely related to group 2 coronaviruses.

Until now five human coronaviruses are known to cause respiratory tract illnesses. HCoV-OC43 and HCoV-229E are responsible for 10–30% of all common colds, and infections occur mainly during the winter and early spring (Larson et al., 1980). During the 2002–2003 winter season, a new human coronavirus, HCoV-NL63, was isolated in The Netherlands (van der Hoek et al., 2004). The recurrent detection of HCoV-NL63 in patient samples worldwide indicates that HCoV-NL63 can be considered as a new important etiologic agent in respiratory tract infections (Arden et al., 2005; Bastien et al., 2005; Moes et al., 2005). The fifth human coronavirus, HCoV-HKU1 was discovered in 2004 by a Chinese group (Woo et al., 2005). Since

* Corresponding author. Tel.: +32 16 337352; fax: +32 16 337340.
** Corresponding author at: Rega Institute for Medical Research, University of Leuven, Minderbroedersstraat 10, 3000 Leuven, Belgium. Tel.: +32 16 347908; fax: +32 16 347900.
E-mail addresses: jan.balzarini@rega.kuleuven.be (J. Balzarini), marc.vanranst@uz.kuleuven.ac.be (M. Van Ranst).

0166-3542/$ – see front matter © 2007 Elsevier B.V. All rights reserved.
doi:10.1016/j.antiviral.2007.03.003

then, this new coronavirus was additionally detected in Australia and France, suggesting a worldwide spread (Sloots et al., 2006; Vabret et al., 2006).

Before the emergence of SARS-CoV, coronavirus research was focused on the veterinary field, where coronaviruses cause devastating epizootics of respiratory or enteric diseases in livestock and poultry. In cats, two coronaviruses are described, the feline infectious peritonitis virus (FIPV) and feline enteric coronavirus (FECV). These feline coronaviruses are spread worldwide and infect domestic cats and other members of the *Felidae* family. An infection with FECV is usually subclinical, except in young kittens where it may cause mild to severe diarrhea (Pedersen et al., 1981). In contrast, FIPV infection causes a chronic and very often fatal peritonitis which is the most important cause of death of infectious origin in cats.

Lectins are natural proteins that target the sugar moieties of a wide variety of glycoproteins. They are widespread among higher plants and are subdivided into seven families of structurally and evolutionarily related proteins (Van Damme et al., 1998). More than a decade ago, plant lectins were reported to inhibit HIV replication in lymphocyte cell cultures through inhibition of virus-cell fusion (Balzarini et al., 1991; Matsui et al., 1990; Hammar et al., 1989; Hansen et al., 1989). Plant lectins are carbohydrate-binding proteins capable of specific recognition and reversible binding to carbohydrates. Initially, it was reported that plant lectins inhibit virus replication by preventing virus adsorption (Muller et al., 1988), but it was later shown that they prevent fusion of HIV particles with their target cells (Balzarini et al., 1991, 1992). In addition to the antiviral effect of mannose- and *N*-acetylglucosamine-specific agglutinins on HIV, an inhibitory effect of these plant lectins was reported on cytomegalovirus infection, respiratory syncytial virus infection and influenza A virus infection *in vitro* (Balzarini et al., 1991, 1992, 2004). The SARS-CoV spike protein is heavily glycosylated and contains 23 putative *N*-glycosylation sites, among which 12 have been described to be effectively glycosylated (Krokhin et al., 2003). One may therefore expect coronavirus infectivity to be inhibited by those lectins that are specific for the glycans present in the spike glycoprotein.

In the present study, we evaluated a panel of 33 carbohydrate-binding proteins, containing mannose, *N*-acetyl glucosamine, glucose, galactose, and *N*-acetyl galactosamine specific plant lectins, for their activity against SARS-CoV and FIPV infection *in vitro*. We demonstrate that the most pronounced anti-coronavirus activity was found mainly among the mannose-binding lectins. Two targets of possible antiviral intervention in the replication cycle of SARS-CoV have been identified.

2. Materials and methods

2.1. Test compounds

The origin and sugar-specificity of the plant lectins used in our study are listed in Table 1. All plant lectins were kindly provided by Prof. Van Damme (University of Gent, Belgium) and were purified as described before (Van Damme et al., 1998, 2002; Chen et al., 2002; Wang et al., 2003). The mannose specific lectin *Hippeastrum hybrid* agglutinin (HHA) was used in the further mechanism of action studies, because of the its availability and its relative good anti-coronavirus activity.

2.2. Cells and virus

The SARS-CoV Frankfurt 1 strain was kindly provided by Prof. Dr. Rabenau from the Johann Wolfgang Goethe University, Frankfurt, Germany. Vero E6 cells ATCC were propagated in minimal essential medium (MEM; Gibco, Life Technologies, Rockville, MD) supplemented with 10% fetal calf serum (FCS; Integro, Zaandam, The Netherlands), 1% L-glutamine (Gibco, Life Technologies, Rockville, MD), and 0.3% sodium bicarbonate (Gibco, Life Technologies, Rockville, MD). Virus-infected cells were maintained at 37 °C in 5% CO_2 in MEM supplemented with 2% FCS. The isolation of FIPV strain 79-1146 was previously described by McKeirnan and co-workers (McKeirnan et al., 2005). Crandell-Reese feline kidney (CrFK) cells were maintained in RPMI-1640 medium (Gibco) supplemented with 10% fetal calf serum (Harlan Sera-Lab Ltd., Loughborough, UK), 2 mM L-glutamine (Gibco), and 0.075% sodium bicarbonate (Gibco). Virus-infected cells were maintained at 37 °C in RPMI-1640 medium supplemented with 2% FCS.

2.3. Virus handling and titration

SARS-CoV culture and assays were carried out in a biosafety level-3 laboratory at the University of Leuven, according to the conditions set out in 'Biosafety in Microbiological and Biomedical Laboratories' (Herman et al., 2004). FIPV was handled in a biosafety level-2 laboratory. The virus titer in the frozen culture supernatant was determined by using a cytopathicity (CPE)-based assay. Briefly, 100 μl of virus in 10-fold serial dilution was added, in quadruplicate, to a subconfluent monolayer of Vero E6 (for SARS-CoV) or CrFK (for FIPV) cells in a 96-well plate. After 3 days of incubation for SARS-CoV, the cells were visually scored for virus-induced CPE. After 4 days of incubation for FIPV, the viability of the virus-infected cells was scored by the tetrazolin-based colorimetric method as described before (Balzarini et al., Antiviral Res., in press, 2006). The limiting dilution end point ($CCID_{50}$/ml) was determined by the Kärber equation (Karber, 1931).

2.4. Antiviral assay

Antiviral activity and cytotoxicity measurements were based on the viability of Vero E6 cells that had been infected (or mock-infected) with 100 $CCID_{50}$ (50% cell culture infective doses) of the SARS-CoV (Keyaerts et al., 2004) and CrFK cells infected (or mock-infected) with 100 $CCID_{50}$ of FIPV in the presence of various concentrations of the test compounds. Three days (SARS-CoV) or 4 days (FIPV) after infection, the number of viable cells was quantified by a tetrazolium-based colorimetric method, in which the reduction of

Table 1
Plant lectins tested for their antiviral activity against SARS-CoV and FIPV

Lectin	Plant species	Common name	Taxonomy	Reference
Man-specific agglutinins				
HHA	*Hippeastrum hybrid*	Amaryllis	Monocot, Amaryllidaceae	Van Damme et al. (1998)
GNA	*Galanthus nivalis*	Snowdrop	Monocot, Amaryllidaceae	Van Damme et al. (1998)
NPA	*Narcissus pseudonarcissus*	daffodil	Monocot, Amaryllidaceae	Van Damme et al. (1998)
LRA	*Lycoris radiata*	Red spider lily	Monocot, Amaryllidaceae	Van Damme et al. (1998)
APA	*Allium porrum*	Leek	Monocot, Alliaceae	Van Damme et al. (1998)
AUA	*Allium ursinum*	Ramsons	Monocot, Alliaceae	Van Damme et al. (1998)
ASA	*Allium sativum*	Garlic	Monocot, Alliaceae	Van Damme et al. (1998)
ASA I	*Allium sativum*	Garlic	Monocot, Alliaceae	Van Damme et al. (1998)
Col O	*Colocasia esculenta*	Taro	Monocot, Araceae	Van Damme et al. (1998)
CA	*Cymbidium hybrid*	Cymbidium orchid	Monocot, Orchidaceae	Van Damme et al. (1998)
LOA	*Listera ovata*	Twayblade	Monocot, Orchidaceae	Van Damme et al. (1998)
EHA	*Epipactis helleborine*	Broad-leaved helleborine	Monocot, Orchidaceae	Van Damme et al. (1998)
TL M I	*Tulipa hybrid*	Tulip	Monocot, Liliaceae	Van Damme et al. (1998)
Morniga M II	*Morus Nigra*	Black mulberry tree	Dicotyl, Moraceae	Van Damme et al. (2002)
GlcNAc-specific agglutinins				
PallGlcNac	*Phragmites australis*	Common reed	Monocot, Gramineae	Van Damme et al. (1998)
Nictaba	*Nicotiana tabacum*	Tabacco plant	Dicot, Solanaceae	Chen et al. (2002)
$(GlcNAc)_n$-specific agglutinins				
UDA	*Urtica dioica*	Stinging nettle	Dicot, Urticaceae c	Van Damme et al. (1998)
Heveine	*Hevea brasiliensis*	Rubber tree	Dicot, Euphorbiaceae	Van Damme et al. (1998)
GalNAc-specific agglutinins				
PMRIP t	*Polygonatum multiflorum tetramer*	Solomon's seal	Monocot, Liliaceae	Van Damme et al. (1998)
BDA	*Bryonia dioica*	White bryony	Dicot, Curcurbitaceae	Van Damme et al. (1998)
Glechoma	*Glechoma hederacea*	Ground ivy	Dicot, Lamiaceae	Wang et al. (2003)
Gal-specific agglutinins				
Morniga G II	*Morus Nigra*	Black mulberry tree	Dicot, Moraceae	Van Damme et al. (2002)
Jacalin	*Artocarpus integrifolia*	Jackfruit	Dicot, Moraceae	Van Damme et al. (1998)
Neu5Acα(2.6)Gal/GalNAc-specific agglutinins				
SNA I	*Sambucus nigra*	Elderberry	Dicot, Sambucaceae	Van Damme et al. (1998)
Man/Glc-specific agglutinins				
Cladistris	*Cladastris lutea*	Yellow wood	Dicot, Fabaceae	Van Damme et al. (1998)
Gal/GalNAc specific agglutinins				
PMRIP m	*Polygonatum multiflorum monomer*	Solomon's Seal	Monocot, Liliaceae	Van Damme et al. (1998)
ML II	*Viscum album*	Mistletoe	Dicotyledoneae, Viscaceae	Van Damme et al. (1998)
GalNAc (>Gal) specific agglutinins				
ML III	*Viscum album*	Mistletoe	Dicotyl, Viscaceae	Van Damme et al. (1998)
GalNAcα(1,3)Gal > GalNAc > Gal-specific agglutinins				
IRA	*Iris hybrid*	Iris	Monocot, Iridaceae	Van Damme et al. (1998)
IRA b	*Iris hybrid*	Iris	Monocot, Iridaceae	Van Damme et al. (1998)
IRA r	*Iris hybrid*	Iris	Monocot, Iridaceae	Van Damme et al. (1998)
Man/GalNAc-specific agglutinins				
TL C II	*Tulipa hybrid*	Tulip	Monocot, Liliaceae	Van Damme et al. (1998)

Monocot: Monocotyledoneae, dicot: Dicotyledoneae, Man: mannose, GlcNac: *N*-acetyl glucosamine, GalNAc: *N*-acetyl galactosamine, Gal: galactose, Neu5Ac: *N*-acetylneuraminic acid.

the 3-(4,5-dimethylthiazol-2-yl)-5-(3-carboxymethoxyphenyl)-2-(4-sulfophenyl)-2*H*-tetrazolium (MTS) dye (CellTiter 96 AQueous One Solution kit, Promega, The Netherlands) by mitochondrial dehydrogenases to a soluble colored formazan was measured in a spectrophotometer (Multiskan EX, Thermo Labsystems, Belgium) at 492 nm. The cytotoxic concentration was defined as the concentration of the compound that reduced cell viability by 50% [50% cytotoxic concentration (CC_{50})], and the antiviral effective concentration was defined as the compound concentration that suppressed the viral cytopathic effect by 50% [50% effective concentration (EC_{50})].

2.5. Real-time RT-PCR

The methodology of the real-time RT-PCR assay has been described previously (Keyaerts et al., 2006). Briefly, a real-time quantitative RT-PCR was designed to measure

copies of the replicase 1B gene of the SARS-CoV genome. Primers spanning a target region of 68 bp were selected: forward primer SARS-FP (5′-CACCCGCGAAG-AAGCTATTC-3′), MGB probe SARS-TP (FAM 5′-TGCGTGGATTGGCTT-3′NFQ-MGB), and reverse primer SARS-RP (5′-TTGCA-TGACAGCCCTCTACATC-3′). A 25 μl RT-PCR was carried out using 5 μl of extracted RNA or standard cRNA, 12.5 μl of one step RT qPCR Mastermix containing ROX as a passive reference (Eurogentec, Seraing, Belgium), 900 nM forward and reverse primer, and 150 nM minor groove binding probe. Amplification and detection were performed in a ABI PRISM 7700 Sequence Detection System (Applied Biosystems, Foster City, CA, USA) under the following conditions: an initial reverse transcription at 48 °C for 30 min, followed by PCR activation at 95 °C for 10 min and 45 cycles of amplification (15 s at 95 °C and 1 min at 60 °C). The threshold cycle represented the refraction cycle number at which a positive amplification was measured, and was set at 10 times the standard deviation of the mean baseline emission calculated for PCR cycles 3–15.

2.6. Time-of-addition assay

Subconfluent monolayers of Vero E6 cells in 96-well plates were infected with 1000 $CCID_{50}$ SARS-CoV. After 20 min of adsorption, cell monolayers were washed five times with PBS. HHA was added in triplicate at a concentration 10-fold above the EC_{50} (i.e. 32 μg/ml), at the time of infection or at a variety of different time points thereafter. Eight hours after infection, a time at which the first viral cycle has already been completed (Keyaerts et al., 2005), supernatants and cells were collected. Viral RNA was extracted using the QIAamp viral RNA kit and Rneasy minikit (Qiagen), respectively to determine the viral RNA-load in the cell supernatant and intracellularly by using the quantitative RT-PCR described above.

2.7. Pre-exposure of cell-free SARS-CoV to the plant lectins prior to infection

In a first set of experiments, a concentrated cell-free SARS-CoV preparation (50 μl) was exposed to 50 μl of 1280, 512, 205, and 82 μg of HHA per ml for 2 h at room temperature (final lectin concentrations of 640, 256, 120, and 41 μg/ml). Then, the drug-exposed virus suspension was diluted such that a final 1000-fold dilution of virus and lectin were used to inoculate Vero E6 cell cultures (1×10^4 cells/well). At day 3 post-infection, virus-induced destruction of the Vero E6 cell cultures was quantified as described above.

2.8. Pre-exposure of Vero E6 cells to the plant lectins prior to infection

Vero E6 cells seeded in 96-well plates were pre-exposed to final HHA concentrations of 640, 256, 64, and 26 μg/ml for 2 h. Then, cell monolayers were washed five times with 200 μl phosphate-buffered saline (PBS). Next, the cells were infected with 100 $CCID_{50}$ SARS-CoV. At day 3 post-infection, the antiviral activity of the plant lectins was determined as described above.

2.9. Virus entry assay

In this assay the inhibitory effects of HHA on virus entry into Vero E6 cells were measured. Therefore, Vero E6 cells (1×10^5 cells/well in a 24 well plate) were incubated with 100 $CCID_{50}$ SARS-CoV in the absence or presence of serial dilutions of the test compound. Two experiments were performed in parallel. In the first setting, the compound was present only during virus attachment (incubation for 60 min at 4 °C). In the second setting, the compound was present during virus attachment and penetration (incubation for 60 min at 37 °C). After this initial incubation, both settings underwent the same procedure. Cells were washed five times with PBS in order to remove the unadsorbed virus particles and the test compound. Subsequently, the 24 well plates were incubated at 37 °C. Eight hours after infection the cells were subjected to a freeze-thaw cycle and cell lysates were collected. Viral RNA was extracted using the QIAamp viral RNA kit and subsequently viral RNA-load quantification was elaborated by using the quantitative RT-PCR described above.

3. Results

3.1. Antiviral activity of plant lectins

A broad range of plant lectins with different specificities were evaluated in a colorimetric cell culture-based assay for their antiviral activity against coronaviruses, namely the SARS-CoV and FIPV. The antiviral activities, represented by their 50% effective concentration or EC_{50}, and the cytotoxic activity in Vero and CrFK cells, represented by their 50% cytotoxic concentration or CC_{50} are shown together with the sugar specificity of the different plant lectins in Table 2. Out of the 33 plant lectins tested against SARS-CoV and FIPV, 15 lectins had antiviral properties against both Coronaviruses; 5 plant lectins were active only against SARS-CoV and 2 lectins showed solely activity against FIPV. Eight lectins were inactive against both SARS-CoV and FIPV. All mannose-binding lectins, except for the lectins isolated from garlic, had anti-coronavirus properties. Cytotoxicity in Vero and CrFK cells was measured in parallel with the determination of the antiviral activity. In general, plant lectins were more toxic to CrFK cells than to Vero E6 cells. The most potent lectin against the SARS-CoV-induced cytopathicity is the mannose-specific plant lectin isolated from leek (APA) with an EC_{50} of 0.45 μg/ml and a selectivity index of >222. In addition, the *N*-acetyl glucosamine-specific lectins isolated from the stinging nettle (UDA) and from the tobacco plant (Nictaba) are also markedly active against the SARS-CoV with a selectivity index of >77 and >59, respectively. For FIPV, the most active lectin is the mannose-specific lectin isolated from the twayblade (LOA) with an EC_{50} of 0.7 μg/ml and a selectivity index of >143 (Table 1).

Table 2
Antiviral activity of plant lectins against SARS-CoV and FIPV replication in Vero and Crandell Feline kidney cells

Lectin	SARS-CoV			FIPV		
	EC_{50} (μg/ml)	CC_{50} (μg/ml)	SI	EC_{50} (μg/ml)	CC_{50} (μg/ml)	SI
Mannose-specific agglutinins						
HHA	3.2 ± 2.8	>100	>31.3	2.6 ± 1.0	>100	>38.5
GNA	6.2 ± 0.6	>100	>16.1	3.9 ± ±2.2	>100	>25.6
NPA	5.7 ± 4.4	>100	>17.5	24 ± 5	>100	>4.2
LRA	48	>100	>2.1	ind	>20	na
APA	0.45 ± 0.08	>100	>222.2	2.0 ± 0.3	17 ± 4	8.5
AUA	18 ± 4	>100	>5.5	16 ± 5	>100	>6.2
ASA	>100	>100	na	>100	>100	na
ASA I	>100	>100	na	>100	>100	na
Col O	>60	63 ± 3	na	2.5 ± 0.6	12 ± 0	4.8
CA	4.9 ± 0.8	>100	>20	4.5 + 2.6	>50	>22
LOA	2.2 ± 1.3	>100	>45.5	0.7 ± 0.3	>100	>142.8
EHA	1.8 ± 0.3	>100	>55.5	1.6 ± 0.9	>100	>62.5
TL M I	22 ± 6	>50	>2.3	ind	>50	na
Morniga M II	1.6 ± 0.5	>100	>62.5	2.9 ± 0.0	11 ± 1	3.8
GlcNAc-specific agglutinins						
PallGlcNac	>100	>100	na	>20	57 ± 1	na
Nictaba	1.7 ± 0.3	>100	>58.8	4.3 ± 1.9	>100	>23.2
$(GlcNAc)_n$-specific agglutinins						
UDA	1.3 ± 0.1	>100	>76.9	3.6 ± 2.3	15 ± 14	4.16
Heveine	>100	>100	na	>100	>100	na
GalNAc-specific agglutinins						
PMRIP t	>100	>100	na	>100	>100	na
BDA	>100	>100	na	>100	>100	na
Glechoma	>100	>100	na	>100	>100	na
Gal-specific agglutinins						
Morniga G II	50 ± 13	>100	>2	11 ± 2	>100	>9.1
Jacalin	>100	>100	na	25 ± 2	>100	>4
Neu5Acα(2.6)Gal/GalNAc-specific agglutinins						
SNA I	>100	>100	na	>100	>100	na
Man/Glc-specific agglutinins						
Cladistris	7.4 ± 0.2	>100	>13.5	17 ± 6	>100	>5.9
Gal/GalNAc specific agglutinins						
PMRIP m	18 ± 13	>100	>5.5	60 ± 5	>100	>1.7
ML II	0.015 ± 0.003	< 0.16	na	>0.008	0.0022 ± 0.005	na
GalNAc (>Gal) specific agglutinins						
ML III	28 ± 11	>100	>12.6	>100	>100	na
GalNAcα(1,3)Gal > GalNAc > Gal-specific agglutinins						
IRA	2.2 ± 0.9	50	22.7	>20	>20	na
IRA b	4.4 ± 3.1	36	8.2	>0.16	0.55 ± 0.23	na
IRA r	3.4 ± 2.0	55	16.2	>0.16	0.49 ± 0.28	na
Man/GalNAc-specific agglutinins						
TL C II	38 ± 0	>50	>1.3	21 ± 1	>50	>2.4

Man: mannose, GlcNac: *N*-acetyl glucosamine, GalNAc: *N*-acetyl galactosamine, Gal: galactose, Neu5Ac: *N*-acetylneuraminic acid, na: no activity, ind: indeterminable.

3.2. Antiviral activity of the mannose-specific lectin of amaryllis (HHA) administered at different time points after coronavirus infection

A time-of-addition assay was performed using the mannose-specific lectin of amaryllis (HHA) to determine its efficacy when added at various times after virus infection. For this purpose, Vero E6 cells were infected with 1000 $CCID_{50}$ SARS-CoV. The virus was allowed to perform a single cycle of replication. The HHA concentration, which is 10 times the $EC_{50,}$ was added at different time points after infection. Viral RNA levels in the cell supernatants and in the cells were determined 8 h post-infection. The measurement of the intracellular viral load shows that the lectins are required at the moment of infection to block the SARS-CoV replication (Fig. 1). When HHA was added at the time of infection, intracellular RNA could still be detected but

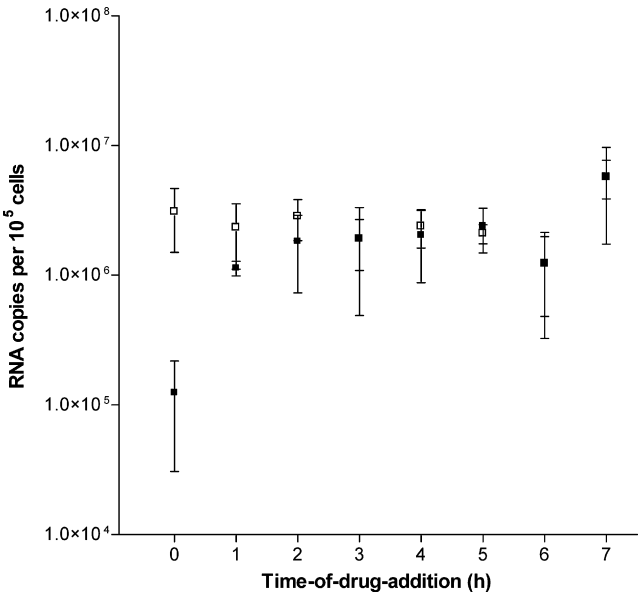

Fig. 1. Intracellular SARS-CoV replication in Vero E6 cells after treatment with HHA concentrations at different time points post-infection (■). Vero E6 cells were infected with 1000 $CCID_{50}$ SARS-CoV FFM-1 at different time-points post-infection HHA (32 μg/ml) is added to the infected cells. The virus control represents infected cells incubated with medium (□). Eight hours after infection, cell supernatants were collected and viral RNA was extracted and quantified by qRT-PCR as described in Section 2. Data are mean values ± S.E.M. of at least three replicates.

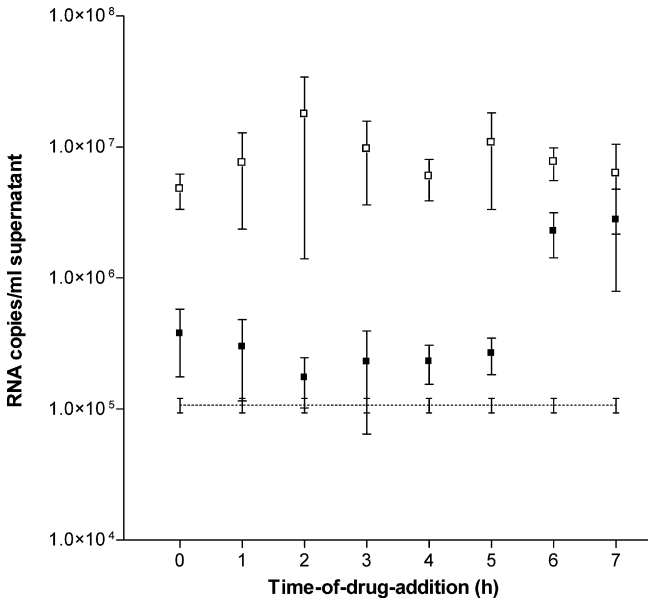

Fig. 2. Extracellular SARS-CoV replication in Vero E6 cells after treatment with HHA at different time points post-infection (■). Vero E6 cells were infected with 1000 $CCID_{50}$ SARS-CoV FFM-1 at different time-points post-infection HHA (32 μg/ml) is added to the infected cells. The virus control represents infected cells incubated with medium (□). Eight hours after infection, cell supernatants were collected and viral RNA was extracted and quantified by qRT-PCR as Section 2. Data are mean values ± S.E.M. of at least three replicates. The dotted line represents the residual background of viral load, that was detected after washing the cells.

the viral load was one log reduced in comparison to the positive control. The extracellular viral load determinations indicate that addition of the lectins to SARS-CoV-infected cells could be delayed up to 5 h without a significant loss of antiviral activity (Fig. 2).

3.3. Virucidal properties of HHA

In order to investigate possible virucidal properties of the plant lectins, two experiments were conducted. In a first set of experiments, the cell-free SARS-CoV was exposed for 2 h to the plant lectin HHA at ca. 200-, 80-, 20-, and eight-fold its EC_{50} concentration (i.e. 640, 256, 102.4, and 41 μg/ml). The drug-exposed virus preparation was then diluted 1000-fold before being used to infect Vero E6 cells. Although reduced infectivity was seen with the highest HHA concentration (i.e. 640 μg/ml), this antiviral effect can not be ascribed to the pre-exposure of the virus to the plant lectin HHA, but was a result of the residual HHA concentration of 0.64 μg/ml, which is only five times below the EC_{50} and offers background protection against viral induced CPE. Thus, pre-exposure of the virus preparations to HHA did not affect the viral replication capacity in the Vero cell cultures. Similarly pre-exposure of the Vero E6 cells, instead of the virus, to the lectins revealed no significantly increased protective activity of the lectins against the virus-induced cytopathicity in pre-treated Vero E6 cells as compared to the SARS-CoV-infected cell cultures that were not pre-incubated with the lectins (data not shown).

3.4. Virus entry assay

To further characterize the mode of action of HHA on its anti-SARS-CoV activity, a virus entry assay was performed. Incubating cells and virus at a low temperature (4 °C), allows most virions to irreversibly attach to the cells, but not penetrate. In a second setting, where cells, compound and virus were incubated for 60 min at 37 °C, both attachment and penetration are achieved. After this initial incubation at 4 °C or at 37 °C, cells were extensively washed with PBS to eliminate residual HHA and unadsorbed virus. Subsequently, the temperature was raised immediately to 37 °C. Results demonstrate that in both situations, HHA showed antiviral activity (Fig. 3). Moreover, when a slower and irreversible attachment was achieved at 4 °C, HHA was two times more active (EC_{50} = 2.5 μg/ml) in comparison to the situation when both attachment and penetration could occur at 37 °C (EC_{50} = 5.2 μg/ml).

4. Discussion

The antiviral activity spectrum of plant lectins varies considerably, depending on the nature of their sugar specificity. In general, the mannose-specific plant lectins are highly effective against coronaviruses. It is also possible that plant lectins with different specificity interfere with different targets necessary for viral entry, depending on the place of the glycans that are targeted. For HIV, it was recently demonstrated that plant lectins with different carbohydrate specificities, i.e. mannose-specific versus *N*-acetylglucosamine-specific, represent carbohydrate-

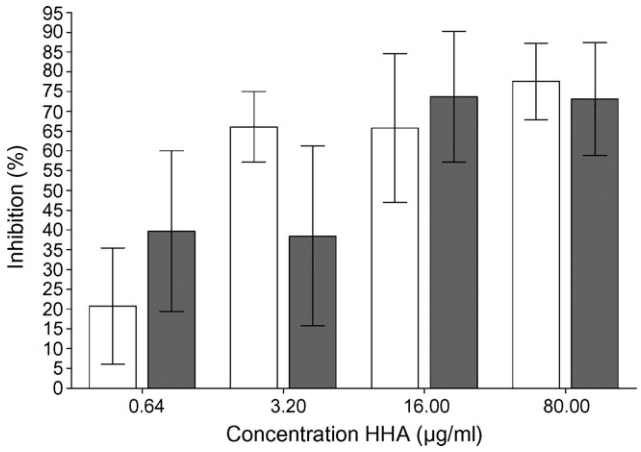

Fig. 3. The inhibitory effects of HHA on virus adsorption to Vero E6 cells are presented as percent protection. Two experiments were performed in parallel. In the first setting (white bars), the compound was present only during virus attachment. In the second setting (black bars), the compound was present during virus attachment and penetration. Data are mean values ± S.E.M. of four replicates.

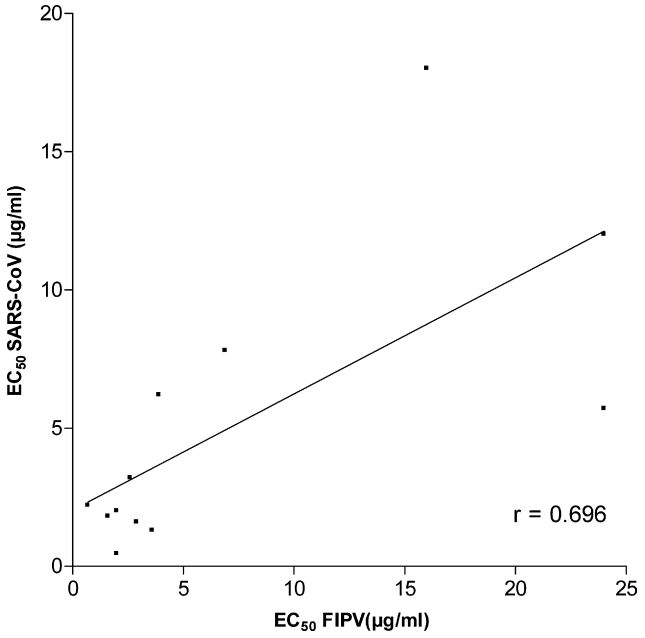

Fig. 4. Calculation of the correlation coefficient between the EC_{50} values of the plant lectins against SARS-CoV on the one hand, and the EC_{50} values of the compounds against FIPV on the other hand, resulted in an *r*-value of 0.38. When only the active mannose-specific lectins were taken into account, an *r*-value of 0.70 was found.

binding agents with a similar mode of antiviral action, but with different genetic barriers (Balzarini et al., 2005).

Out of 33 plant lectins evaluated, 15 showed antiviral properties against both SARS-CoV and FIPV, and 8 plant lectins showed no anti-coronavirus activity. The lectins with anti-coronaviral activity included mannose-, glucose-, galactose-, *N*-acetyl glucosamine- and *N*-acetyl galactosamine-specific agglutinins In general plant lectins were more toxic to CrFK cells than to Vero E6 cells. This could partly explain some differences between the SARS-CoV activity and FIPV activity of plant lectins. Most of the lectins that were not active against FIPV were too toxic for the CrFK cells. The most prominent anti-coronavirus activity was found among the mannose-specific plant lectins. In the SARS-CoV spike protein there are 12 *N*-glycosylation sites. The sugars attached to four of these *N*-glycosylation sites have been identified (Krokhin et al., 2003). Two of the four sugars were found to be high-mannose type glycans, whereas the other two showed complex glycan structures (Krokhin et al., 2003). The presence of high-mannose type glycans can explain the potent anti-SARS-CoV activity of mannose-specific plant lectins. When we compare the activity spectrum of the plant lectins against coronaviruses with their activity spectrum against HIV, only the mannose-specific plant lectins, with the exception of UDA, which is a *N*-acetyl glucosamine-specific lectin, possess antiviral activity against HIV (Balzarini et al., 1991, 1992). Thus, the carbohydrate spectrum of plant lectins that inhibit virus infection is broader for coronaviruses than for HIV.

Calculation of the correlation coefficient between the EC_{50} values of the plant lectins against SARS-CoV on the one hand, and the EC_{50} values of the compounds against FIPV on the other hand, resulted in an *r*-value of 0.38. When only the active mannose-specific lectins were taken into account, a much higher *r*-value of 0.70 was calculated (Fig. 4). Furthermore, a marked correlation was found when the correlation coefficient between the anti-HIV activity of the plant lectins (Balzarini et al., 1991, 1992), and their anti-FIPV or anti-SARS-CoV activity was calculated (*r*-values were found to be 0.55 and 0.52, respectively).

Plant lectins are known to possess virucidal properties against HIV, and may therefore qualify as HIV microbicides (Balzarini et al., 2004). In contrast to HIV, the plant lectins did not show marked virucidal properties against the SARS-CoV, neither when they were pre-incubated with the cells, nor when pre-incubated with the virus. This can be due to a lower binding affinity (on-rate) of the plant lectins to the coronavirus envelope glycans and/or a faster off-rate of the plant lectins from the coronavirus envelope glycans.

To elucidate the mechanism of antiviral intervention of the plant lectins, a time-of-addition assay was elaborated using the mannose-specific lectin of the amaryllis (HHA). The lectin was added to the infected cell cultures at different time-points post-infection. At 8 h post-infection, the SARS-CoV viral load was quantified intracellularly and extracellularly. A marked difference was noted between these two measurements. The intracellular viral RNA-load could only be efficiently reduced when the lectin was added at the time of infection, indicating that the plant lectins interact with an early step in the viral replication cycle. In general, the SARS-CoV entry starts with the attachment of the virus to its specific receptor ACE2 on the cell surface. The receptor binding subsequently induces the viral envelope protein to undergo conformational changes that mediate fusion between the viral and cellular membranes (Doms, 2004). The coronavirus spike glycoprotein is responsible for these two steps in the coronavirus entry process. Since each step of the viral entry pathway is a potential target for antiviral agents, entry inhibitors fall into several categories. A first class consists of inhibitors that bind to the ACE2 receptor, a second category comprises entry inhibitors

that bind to the virus and prevent it from interacting with its receptors and a third group of inhibitors can hamper the conformational changes, resulting in the inhibition of SARS-CoV fusion with the target cell. In order to distinguish between these categories of entry inhibitors more in-depth studies were conducted. The virus entry assay showed that HHA was active when incubating the cells and virus at 4 °C. This low temperature incubation allows most virions to irreversibly attach to the cells, but not to penetrate the cells. Moreover, when this slower and irreversible attachment was achieved at 4 °C, HHA was two times more active (EC_{50} = 2.5 μg/ml) in comparison to attachment and penetration at 37 °C (EC_{50} = 5.2 μg/ml). This observation indicates that this compound most probably interferes with virus attachment. To elucidate if HHA is an ACE2 receptor inhibitor or an entry inhibitor which binds the virus, and prevent it in this way from interacting with its receptor, we pre-incubated HHA with either the SARS-CoV or with the cells. Pre-incubation of HHA with the virus did not provide inhibition of virus replication, nor did the pre-incubation of HHA with the cells. These pre-incubation experiments did not help us to understand the mechanism of action of the plant lectins.

Interestingly, the results of the extracellular viral RNA quantification also points to an intervention at a late step in the replication cycle around 5 h post-infection. Huang and colleagues observed that the presence of the spike protein in a pseudoparticle is necessary for budding and formation of a corona-like structure (Huang et al., 2004). This indicates that the spike protein is likely to be important not only for viral attachment and fusion, but also for maturation and egress from cells. Earlier we demonstrated that one SARS-CoV replication cycle takes 6 h to complete in Vero E6 cells (Keyaerts et al., 2005). Therefore, inhibition of extracellular viral RNA-load up to 5 h post-infection suggests interference at the level of exocytosis or egress from the cell. Taken together, we could clearly demonstrate that the plant lectins interact both at virus entry and at virus release, a phenomenon that has never been observed for other viruses, including HIV.

In conclusion, we identified a variety of plant lectins as antiviral compounds against the SARS-CoV and the FIPV. The lectins most probably interfere with the glycans on the spike protein during virus entry and virus release. In view of the fact that the SARS-CoV discovery led to the identification of two new human coronaviruses, HCoV-NL63 and HCoV-HKU1, both of which are associated with serious lower respiratory diseases, the search for efficient anti-coronavirus compounds becomes more important. Our findings on the selective and potent anti-coronavirus activity of plant lectins should trigger further research on the discovery of other carbohydrate-binding agents, including synthetic low-molecular-weight compounds.

Acknowledgments

We would like to thank all the colleagues of the laboratory of Clinical & Epidemiological Virology, Department of Microbiology and Immunology, Rega Institute for Medical Research, University of Leuven, Belgium, for helpful comments and discussion. We thank Lizette van Berckelaer for excellent technical assistance. This work is part of the activities of the Euro-Asian SARS-DTV Network (SP22-CT-2004-511064) supported by the European Commission specific research and technological development program "Integrating and Strengthening the European Research Area" and the R. Descartes Prize-2001 of the European Commission and the Centers of Excellence of the K.U. Leuven (to JB.). This work was supported by a postdoctoral fellowship of the Research Fund K.U. Leuven to Leen Vijgen.

References

Arden, K.E., Nissen, M.D., Sloots, T.P., Mackay, I.M., 2005. New human coronavirus, HCoV-NL63, associated with severe lower respiratory tract disease in Australia. J. Med. Virol. 75, 455–462.

Balzarini, J., Schols, D., Neyts, J., Van Damme, E., Peumans, W., De Clercq, E., 1991. Alpha-(1-3)- and alpha-(1-6)-D-mannose-specific plant lectins are markedly inhibitory to human immunodeficiency virus and cytomegalovirus infections in vitro. Antimicrob. Agents Chemother. 35, 410–416.

Balzarini, J., Neyts, J., Schols, D., Hosoya, M., Van Damme, E., Peumans, W., De Clercq, E., 1992. The mannose-specific plant lectins from cymbidium hybrid and epipactis helleborine and the (*N*-acetylglucosamine)*n*-specific plant lectin from Urtica dioica are potent and selective inhibitors of human immunodeficiency virus and cytomegalovirus replication in vitro. Antiviral Res. 18, 191–207.

Balzarini, J., Hatse, S., Vermeire, K., Princen, K., Aquaro, S., Perno, C.F., De Clercq, E., Egberink, H., Vanden Mooter, G., Peumans, W., Van Damme, E., Schols, D., 2004. Mannose-specific plant lectins from the Amaryllidaceae family qualify as efficient microbicides for prevention of human immunodeficiency virus infection. Antimicrob. Agents Chemother. 48, 3858–3870.

Balzarini, J., Van Laethem, K., Hatse, S., Froeyen, M., Peumans, W., Van Damme, E., Schols, D., 2005. Carbohydrate-binding agents cause deletions of highly conserved glycosylation sites in HIV GP120: a new therapeutic concept to hit the achilles heel of HIV. J. Biol. Chem. 280, 41005–41014.

Bastien, N., Anderson, K., Hart, L., Van Caeseele, P., Brandt, K., Milley, D., Hatchette, T., Weiss, E.C., Li, Y., 2005. Human coronavirus NL63 infection in Canada. J. Infect. Dis. 191, 503–506.

Chen, Y., Peumans, W.J., Hause, B., Bras, J., Kumar, M., Proost, P., Barre, A., Rouge, P., Van Damme, E.J., 2002. Jasmonic acid methyl ester induces the synthesis of a cytoplasmic/nuclear chito-oligosaccharide binding lectin in tobacco leaves. FASEB J. 16, 905–907.

Doms, R.W., 2004. Viral entry denied. N. Engl. J. Med. 351, 743–744.

Gonzalez, J.M., Gomez-Puertas, P., Cavanagh, D., Gorbalenya, A.E., Enjuanes, L., 2003. A comparative sequence analysis to revise the current taxonomy of the family Coronaviridae. Arch. Virol. 148, 2207–2235.

Hammar, L., Eriksson, S., Morein, B., 1989. Human immunodeficiency virus glycoproteins: lectin binding properties. AIDS Res. Hum. Retroviruses 5, 495–506.

Hansen, J.E., Nielsen, C.M., Nielsen, C., Heegaard, P., Mathiesen, L.R., Nielsen, J.O., 1989. Correlation between carbohydrate structures on the envelope glycoprotein gp120 of HIV-1 and HIV-2 and syncytium inhibition with lectins. AIDS 3, 635–641.

Herman, P., Verlinden, Y., Breyer, D., Van Cleemput, E., Brochier, B., Sneyers, M., Snacken, R., Hermans, P., Kerkhofs, P., Liesnard, C., Rombaut, B., Van Ranst, M., Van Der Groen, G., Goubau, P., Moens, W., 2004. Biosafety risk assessment of the severe acute respiratory syndrome (SARS) Coronavirus and containment measures for the diagnostic and research laboratories. Appl. Biosafety 9, 128–142.

Huang, Y., Yang, Z.Y., Kong, W.P., Nabel, G.J., 2004. Generation of synthetic severe acute respiratory syndrome coronavirus pseudoparticles: implications for assembly and vaccine production. J. Virol. 78, 12557–12565.

Karber, G., 1931. Beitrag zur kollektiven behandlungpharmakologischer Reihenversuche. Arch. Exp. Pathol. Pharmakol. 162, 480–483.

Keyaerts, E., Vijgen, L., Maes, P., Neyts, J., Van Ranst, M., 2004. In vitro inhibition of severe acute respiratory syndrome coronavirus by chloroquine. Biochem. Biophys. Res. Commun. 323, 264–268.

Keyaerts, E., Vijgen, L., Maes, P., Neyts, J., Van Ranst, M., 2005. Growth kinetics of SARS-coronavirus in Vero E6 cells. Biochem. Biophys. Res. Commun. 329, 1147–1151.

Keyaerts, E., Vijgen, L., Maes, P., Duson, G., Neyts, J., Van Ranst, M., 2006. Viral load quantitation of SARS-coronavirus RNA using a one-step real-time RT-PCR. Int. J. Infect. Dis. 10, 32–37.

Krokhin, O., Li, Y., Andonov, A., Feldmann, H., Flick, R., Jones, S., Stroeher, U., Bastien, N., Dasuri, K.V., Cheng, K., Simonsen, J.N., Perreault, H., Wilkins, J., Ens, W., Plummer, F., Standing, K.G., 2003. Mass spectrometric characterization of proteins from the SARS virus: a preliminary report. Mol. Cell Proteomics. 2, 346–356.

Larson, H.E., Reed, S.E., Tyrrell, D.A., 1980. Isolation of rhinoviruses and coronaviruses from 38 colds in adults. J. Med. Virol. 5, 221–229.

Matsui, T., Kobayashi, S., Yoshida, O., Ishii, S., Abe, Y., Yamamoto, N., 1990. Effects of succinylated concanavalin A on infectivity and syncytial formation of human immunodeficiency virus. Med. Microbiol. Immunol. (Berl) 179, 225–235.

McKeirnan, A.J., Evermann, J.F., Hargis, A., Ott, R.L., 2005. Isolation of feline coronaviruses from two cats with diverse disease manifestations. Feline Pract. 11, 17–20.

Moes, E., Vijgen, L., Keyaerts, E., Zlateva, K., Li, S., Maes, P., Pyrc, K., Berkhout, B., van der, H.L., Van Ranst, M., 2005. A novel pancoronavirus RT-PCR assay: frequent detection of human coronavirus NL63 in children hospitalized with respiratory tract infections in Belgium. BMC. Infect. Dis. 5, 6.

Muller, W.E., Renneisen, K., Kreuter, M.H., Schroder, H.C., Winkler, I., 1988. The D-mannose-specific lectin from Gerardia savaglia blocks binding of human immunodeficiency virus type I to H9 cells and human lymphocytes in vitro. J. Acquir. Immune. Defic. Syndr. 1, 453–458.

Pedersen, N.C., Boyle, J.F., Floyd, K., Fudge, A., Barker, J., 1981. An enteric coronavirus infection of cats and its relationship to feline infectious peritonitis. Am. J. Vet. Res. 42, 368–377.

Rota, P.A., Oberste, M.S., Monroe, S.S., Nix, W.A., Campagnoli, R., Icenogle, J.P., Penaranda, S., Bankamp, B., Maher, K., Chen, M.H., Tong, S., Tamin, A., Lowe, L., Frace, M., DeRisi, J.L., Chen, Q., Wang, D., Erdman, D.D., Peret, T.C., Burns, C., Ksiazek, T.G., Rollin, P.E., Sanchez, A., Liffick, S., Holloway, B., Limor, J., McCaustland, K., Olsen-Rasmussen, M., Fouchier, R., Gunther, S., Osterhaus, A.D., Drosten, C., Pallansch, M.A., Anderson, L.J., Bellini, W.J., 2003. Characterization of a novel coronavirus associated with severe acute respiratory syndrome. Science 300, 1394–1399.

Sloots, T.P., McErlean, P., Speicher, D.J., Arden, K.E., Nissen, M.D., Mackay, I.M., 2006. Evidence of human coronavirus HKU1 and human bocavirus in Australian children. J. Clin. Virol. 35, 99–102.

Vabret, A., Dina, J., Gouarin, S., Petitjean, J., Corbet, S., Freymuth, F., 2006. Detection of the new human coronavirus HKU1: a report of 6 cases. Clin. Infect. Dis. 42, 634–639.

Van Damme, E., Peumans, W., Pusztai, A., Bardocz, S., 1998. Handbook of Plant Lectins: Properties and Biomedical Applications. John Wiley & Sons, Chichester, West Sussex, England.

Van Damme, E.J., Hause, B., Hu, J., Barre, A., Rouge, P., Proost, P., Peumans, W.J., 2002. Two distinct jacalin-related lectins with a different specificity and subcellular location are major vegetative storage proteins in the bark of the black mulberry tree. Plant Physiol. 130, 757–769.

van der Hoek, L., Pyrc, K., Jebbink, M.F., Vermeulen-Oost, W., Berkhout, R.J., Wolthers, K.C., Wertheim-van Dillen, P.M., Kaandorp, J., Spaargaren, J., Berkhout, B., 2004. Identification of a new human coronavirus. Nat. Med. 10, 368–373.

Wang, W., Peumans, W.J., Rouge, P., Rossi, C., Proost, P., Chen, J., Van Damme, E.J., 2003. Leaves of the Lamiaceae species Glechoma hederacea (ground ivy) contain a lectin that is structurally and evolutionary related to the legume lectins. Plant J. 33, 293–304.

Woo, P.C., Lau, S.K., Chu, C.M., Chan, K.H., Tsoi, H.W., Huang, Y., Wong, B.H., Poon, R.W., Cai, J.J., Luk, W.K., Poon, L.L., Wong, S.S., Guan, Y., Peiris, J.S., Yuen, K.Y., 2005. Characterization and complete genome sequence of a novel coronavirus, coronavirus HKU1, from patients with pneumonia. J. Virol. 79, 884–895.